A Vision-Based Collision Warning System by Surrounding Vehicles Detection

Bing-Fei Wu[1], Ying-Han Chen[1], Chih-Chun Kao[1], Yen-Feng Li[1] and Chao-Jung Chen[1]
[1] Department of Electrical Engineering,
National Chiao Tung University, Hsinchu, Taiwan
[e-mail: {bwu, winand, kevinkao, takolyf, cjchen}@cssp.cn.nctu.edu.tw]
*Corresponding author: Ying-Han Chen

Received October 12, 2011; revised March 2, 2012; accepted April 5, 2012; published April 25, 2012

Abstract

To provide active notification and enhance drivers' awareness of their surroundings, a vision-based collision warning system that detects and monitors surrounding vehicles is proposed in this paper. The main objective is to prevent possible vehicle collisions by monitoring the status of surrounding vehicles, including the distance to the other vehicles in front, behind, to the left and to the right sides. In addition, the proposed system collects and integrates this information to provide advisory warnings to drivers. To offer the correct notification, an algorithm based on features of edge and morphology to detect vehicles is also presented. The proposed system has been implemented in embedded systems and evaluated on real roads in various lighting and weather conditions. The experimental results indicate that the vehicle detection ratios were higher than 97% in the daytime, and appropriate for real road applications.

Keywords: Vision, blind spots, vehicle detection, collision warning, surrounding monitoring

A preliminary version of this paper appeared in IEEE SMC 2008, Oct. 12-15, Singapore. This version includes algorithm explanation and supporting implementation results on the driving assistance system. This research was supported by a research grant from the National Science Council [NSC 100-2221-E-009-042-].

http://dx.doi.org/10.3837/tiis.2012.04.015

1. Introduction

Recently, the number of deaths resulting from traffic accidents has sharply increased, with careless driving identified as the main factor behind such accidents. Drivers usually focus on the vehicles in front of them, and only occasionally examine the status of those at their sides and behind them. While driving, a motorist needs to pay attention to the surrounding traffic, dashboard displays, and a variety of information on the road, such as traffic lights and road signs. S/he may even be inclined to talk to passengers and talk on a cell phone. These are all factors that can cause the driver to become distracted, and may result in collisions with other vehicles or, at the very least, deviation from the lane. These misfortunes can be avoided if the drivers are notified ahead of time with warning messages. Therefore, knowledge of surroundings plays an important role in safe driving. In our research, we are developing technologies that provide drivers with information on the status of vehicles surrounding them at the front, to the rear, and on both sides in order to enhance their awareness.

Many researchers have focused on the development of advanced driver assistance systems (ADAS) to improve driving safety and driver performance. Some researches focus on the inter-vehicle communication technologies [1], while others aim at assistance systems for the vehicle itself. Projects such as VaMP [2], GOLD [3], and ARGO [4] have also proposed to develop various functions to assist drivers. To develop an intelligent vehicle, sensors are necessary and essential for collecting information on the environment. Two kinds of sensors, active and passive [5], are widely used in the development of ADAS. Active sensors require input energy from a source other than that which is being sensed. Radar-based [6], laser-based [7], and acoustic-based [8] sensors are all active sensors. Wijesoma et al. [9] used laser radars (ladar) to scan road curbs to obtain the status of lanes. Their system triggers warning messages when the driving status is identified as irregular. Sheu et al. [10] proposed a distance and direction awareness system for intelligent vehicles (DDAS) that provides information on the surroundings using smart antennas so as to enable drivers to maintain proper behavior. In the advanced safety vehicles project of Toyota [11], the driver has to wear a wristband to measure his/her heart rate, while Mitsubishi is reportedly utilizing steering wheel sensors in their AVS system [12] to assess the vehicle's behavior and thereby determine if a driver is drowsy or not. However, these systems may be too expensive as they require more equipment, leading to an increase in cost and other limitations compared to image-based processing systems.

Other kinds of driver assistance systems proposed are based on machine vision and only require several cameras and processing units to compute the algorithms. Some research focus on the assessment of a driver's condition, such as level of drowsiness and vigilance. Hayami et al. [13] used eye status to monitor drivers' condition to determine whether they were drowsy. To improve accuracy and robustness, six parameters were calculated and combined using a fuzzy classifier to infer the level of inattentiveness of the driver [12]. These methods primarily resolve the problem of possible hazardous situations caused when drivers fall asleep. However, even when drivers do not doze, dangerous actions such as lane departure, and too short a distance between cars may still occur due to other factors.

The detection of vehicles and lane markings is another approach that can be utilized by ADAS to overcome the above shortcomings resulting from only detecting a driver's behavior. Three kinds of methods, motion-based, stereo-based, and knowledge-based, are widely used to detect objects of interest in the image. Motion-based methods estimate the motion of the ground plane and then detect those obstacles whose motions differ from that of the ground

[14][15][16]. In these methods, it is necessary to make a tracking trajectory about the motion among images for large displacements and, as a consequence, the assumption of rectilinear motions in optical flow-based methods is invalid. Since the scenes vary very much among the images, it is difficult to identify the pixel correspondence. If the size of the search area is too small, the correct matching for the corresponding pixels may be missed. On the other hand, if the size is too large, too many possibilities may exist. In addition, motion-based approaches incur expensive computational costs.

Stereo-based approaches take advantage of inverse perspective mapping (IPM) [17] to estimate the locations of vehicles and obstacles in images. Bertozzi et al. [3] computed the IPM both from the left and right cameras. By comparing the two IPMs, they were able to find objects that were not on the ground plane. Using this information, they determined the free space in front of the vehicle. In [18], the IPM was used to wrap the left image to the right image. Knoeppel et al. [19] developed a stereo-system that detects vehicles up to 150 m away. The main problem with stereo-based methods is that they are sensitive to the recovered camera parameters. Accurate and robust methods are required to recover these parameters because of vehicle vibrations due to vehicle motion or windy conditions [20]. Principal component analysis (PCA) templates were used to recover the structure and posture of vehicles in [21]; while Haar wavelet features were extracted to match with template features in [22]. PCA templates and Haar wavelet features need models that match different vehicle types so storing those models in a memory-limited embedded system is impractical.

Knowledge-based methods employ a priori knowledge to locate the vehicles in an image. Symmetry, color, shadow, and geometrical features are all representative information used in knowledge-based methods. Symmetry is one of the main signatures, and has been used for vehicle detection in several studies [23][24]. Although the use of color information takes more effort than mono images, it is a very useful feature for obstacle detection. Several prototype systems have been developed to follow lanes and roads [25], or segment vehicles from background [26]. Shadow information is used as a feature for vehicle detection in [27]. Because the area underneath a vehicle is (usually) distinctly darker than any other areas on a road, the vehicle can be located from the position of its shadow. However, the intensity of the shadow depends on the illumination of the image, and a fixed threshold cannot be used to detect the shadow. An adaptive threshold is necessary for different environments.

A vehicle contains many horizontal and vertical structures, such as a rear window and a bumper. The use of constellations of vertical and horizontal edges is a strong feature to identify a vehicle [28]. Matthews et al. [29] used edge detection to find strong vertical edges, and to localize the left and right positions of a vehicle. They used a triangular filter to smooth the edges, and searched the local maximum peaks of the vertical edge to find the left/right boundary of a vehicle. A coarse-to-fine search method using edge information to detect distant cars was proposed in [30]. The coarse search checked the entire image to see if prominent edges exist in order to decide on a refined region. After acquiring the result of the coarse search, the refined search process would then start in that region. In [31], both vertical and horizontal edges are used and two constraint filters—rank filter and attached line edge filter—are utilized to segment vehicles from their background. Bucher et al. [32] used detected lane information to search for candidate vehicles by scanning each lane starting from the bottom to a certain vertical position. The candidate vehicles were obtained if a strong horizontal edge segment within the lane was found. If the prior knowledge is designed reasonably well, knowledge-based methods can also obtain robust results similar to the above-mentioned methods without any significant increase in complexity. Therefore, our system primarily uses knowledge-based methods to realize vehicle detection.

In this study, a vision-based collision warning system that detects and monitors surrounding vehicles is proposed. Our work has been implemented in an embedded system. The main objective is to monitor the driver's surroundings and actively provide real-time notification in order to avoid possible collisions. The vehicle is equipped with four cameras to capture images in front, at the rear, and in the blind spots of the vehicle, as depicted in **Fig. 1**.

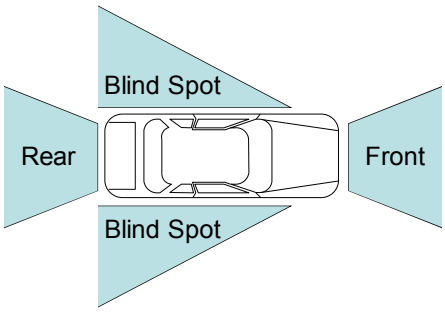

Fig. 1. The areas monitored by the proposed system

Both lane markings and vehicles are recognized, and the distances between the host vehicle and surrounding vehicles are estimated. The information is collated and warning alarms are raised when the system considers that the driver is in a dangerous situation. The main contribution of the proposed system is the provision of driver protection in all aspects, and the reduction of driver stress.

The remainder of this paper is organized as follows: Section 2 presents the camera model and explains how to build the relationship between the image and world coordinates. Section 3 addresses the algorithm used for vehicle detection in the front, at the rear, and in the blind spots. Section 4 presents experimental results obtained from the evaluation of the system under various road and weather conditions. Finally, a brief conclusion and a discussion of possible implications are given in Section 5.

2. Camera Model for Image and World Coordinates Transformation

To know the status of the surrounding vehicles, 3D to 2D projection is necessary for the vision-based system. The scene point (X_c, Y_c, Z_c) in the camera coordinate system is captured by a camera and projected onto the image pixels in the image coordinate system, as illustrated in **Fig. 2**.

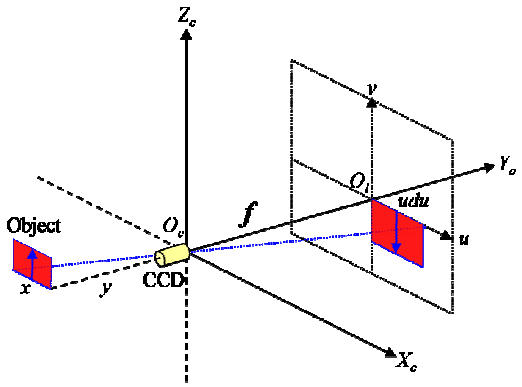

Fig. 2. The camera coordinate system

The projection relationship from camera coordinates (X_c, Y_c, Z_c) to the image plane (u, v) is shown as follows:

$$u = e_u \cdot X_c / Y_c \tag{1}$$

$$v = e_u \cdot Z_c / Y_c \tag{2}$$

where (u, v) and (X_c, Y_c, Z_c) are the image and camera coordinates, respectively. e_u and e_v indicate the intrinsic parameters of the camera and are denoted as (3) and (4), respectively.

$$e_u = f / du \tag{3}$$

$$e_v = f / dv \tag{4}$$

du and dv represent the physical width and height of an image pixel, respectively, while f is the focal length of the camera. (1) and (2) are the non-linear equations that transform the 3D scene point of the camera into 2D image pixels. **Fig. 3** illustrates the relationship between the camera and world coordinate systems.

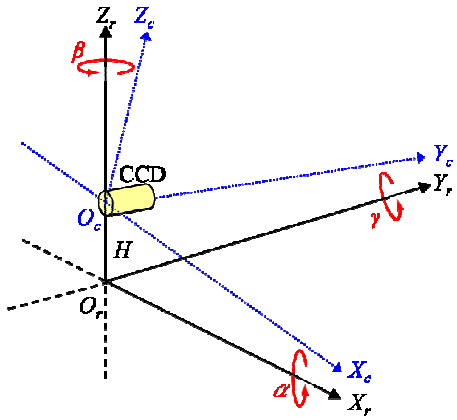

Fig. 3. The camera and world coordinate systems

The points in the world coordinate system are indicated as (X_r, Y_r, Z_r). In **Fig. 3**, α represents the tilt angle; β, the pan angle; γ, the swing angle; and H, the height of the camera. The points in the world coordinate can transform to the image coordinate by means of translation and rotation. In our system, the tilt angle α and the swing angle γ are set at 0° when the cameras are installed. For front and rear vehicle detection, the cameras are installed on the windscreen of the vehicle. Hence, the pan angle β is set at 0°. The projection equations from the world space to the image plane are (5) and (6) below.

$$u = e_u \cdot X_r / Y_r \tag{5}$$

$$v = e_u \cdot \left(Z_r - H\right) / Y_r \tag{6}$$

On the other hand, for blind spot vehicle detection, the cameras are installed on the side mirrors of the vehicle. The pan angle β has to be considered when the cameras are installed. The projection equations from the world space to the image plane become

$$u = e_u \cdot \frac{\cos\beta \cdot X_r - \sin\beta \cdot Y_r}{\sin\beta \cdot X_r + \cos\beta \cdot Y_r} \tag{7}$$

$$v = e_v \cdot \frac{Z_r - H}{\sin\beta \cdot X_r + \cos\beta \cdot Y_r} \tag{8}$$

In the global coordinates, the road surface is modeled as a plane with an inclined angle θ. The relationship between Y_r and Z_r becomes

$$Z_r = Y_r \cdot \tan\theta = Y_r \cdot m_\theta \tag{9}$$

where m_θ is represented as $\tan\theta$ for convenience. Next, we combine (5), (6), and (9) to produce

$$X_r = \frac{uH}{e_v m_\theta - v} \cdot \frac{e_u}{e_v} \tag{10}$$

$$Y_r = \frac{e_v H}{e_v m_\theta - v} \tag{11}$$

$$Z_r = \frac{e_v H m_\theta}{e_v m_\theta - v} \tag{12}$$

Using (10), (11), and (12), the points (u, v) in the image coordinate system can be transformed to corresponding points in the world coordinate (X_r, Y_r, Z_r). When the system detects the position of the vehicle to the front or rear side, the distance can be calculated using the above formulas.

For blind spot vehicle detection, by combining (7), (8), and (9) the formulas become as follows.

$$X_r = \frac{\mathrm{H}\left(\sin\beta + \cos\beta \dfrac{u}{e_u}\right)}{m_\theta\left(\cos\beta - \sin\beta \dfrac{u}{e_u}\right) - \dfrac{v}{e_v}} \tag{13}$$

$$Y_r = \frac{\mathrm{H}\left(\cos\beta - \sin\beta \dfrac{u}{e_u}\right)}{m_\theta\left(\cos\beta - \sin\beta \dfrac{u}{e_u}\right) - \dfrac{v}{e_v}} \tag{14}$$

$$Z_r = \frac{\mathrm{H}\left(\cos\beta - \sin\beta \dfrac{u}{e_u}\right)}{\left(\cos\beta - \sin\beta \dfrac{u}{e_u}\right) - \dfrac{v}{e_v}} \tag{15}$$

We observe that whether the derived formulas contain the pan angle β or not, parameter m_θ still has to be determined. Because an incorrect parameter affects the accuracy of the result, calibration is necessary in the system. To achieve this purpose, we model the lane geometry in the form of a polynomial as follows

$$X_r = kY_r^2 + mY_r + b \tag{16}$$

By substituting (10)–(12) into (9), parameter m_θ can be derived from coefficient m. Thence, with the verified data (X_r, Y_r), coefficients k, m, and b can be determined by the weighted least squares (WLS) approximation. This information can further be used for lane marking detection—which was detailed in our previous work [33]. In this paper, the results of the lane model and lane marking are essential for vehicle detection. A detailed explanation follows in Section 3.

3. Vehicle Detection and Surroundings Monitoring

3.1 Algorithms for Front and Rear Collision Warning

In this section, the vehicle detection algorithm is presented. The goal of front vehicle detection is to enable drivers to utilize the vision-based object detection algorithm to detect the front vehicle and its relative position. Lane information is utilized in the vehicle detection process. Candidate vehicles are sought in the host lane. The vehicle detection procedure is activated after lane detection. There are two major detection modes: *Single Mode* and *Continuous Mode*. In the vehicle detection mode, the settings for the different modes are different. The vehicle detection process flow is demonstrated in **Fig. 4**.

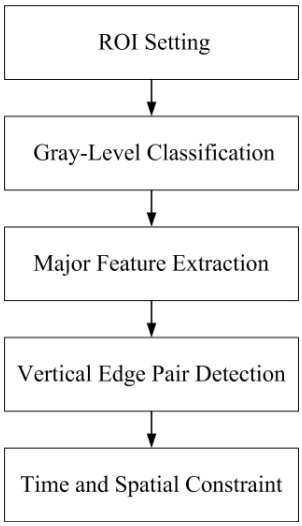

Fig. 4. The vehicle detection process flow

A. ROI Setting Algorithms

1) ROI Setting in Single Mode

In Single Mode, there is no previous vehicle information for reference. To achieve better system performance, ROI Setting in the vehicle detection algorithm is bounded by lane detection. After lane detection, the host lane region is identified, as depicted in **Fig. 5-(a)**. In this region, three searching lines are assumed for vehicle detection, as shown in **Fig. 5-(b)**, where $B_1 = (A_1 + A_2) / 2$, $C_1 = (A_1 + B_1) / 2$ and $C_2 = (B_1 + A_2) / 2$.

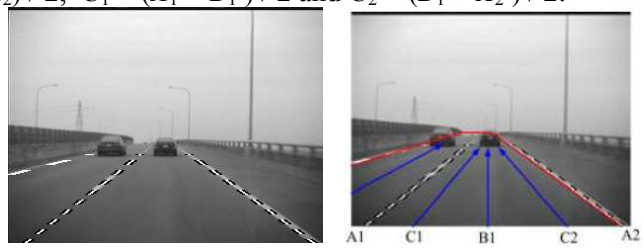

(a) (b)

Fig. 5. (a) The lane detection result (b) The lines searching for vehicles

2) ROI Setting in Continuous Mode

In this mode, previous vehicle information is obtained, as shown in **Fig. 6-(a)**. If the frame rate

is sufficiently high, the vehicle position in the image only varies a tiny distance. Therefore, the position of the vehicle in the current frame can be predicted from the previous frame. The search region is arranged as shown in **Fig. 6-(b)**.

(a) (b)

Fig. 6. (a) The detected vehicle (b) The search region in Continuous Mode

B. Gray-Level Classification

The features of a vehicle in different weather are distinct. Therefore, it is necessary to obtain a threshold value automatically in order to achieve all-weather detection. The most important feature in the vehicle detection process is the gray-level value. From observation, it can be seen that the road surface occupies the most area in the image. Hence, the threshold value can be set automatically by classifying the gray-level of the road surface. According to the lane detection result, the search region is arranged near to the lane markings in **Fig. 7-(a)**. The gray-level distribution of the yellow region is illustrated in **Fig. 7-(b)**. Thus, the threshold value for the vehicle detection process is set automatically.

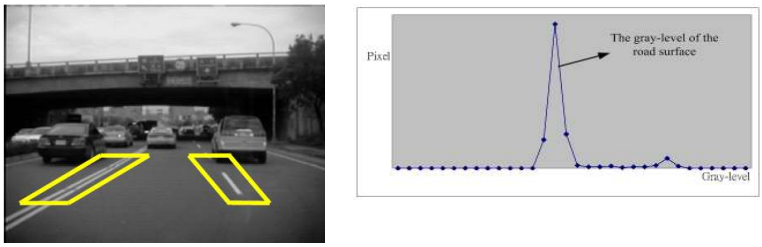

(a) (b)

Fig. 7. (a) The region of classification (b) The gray-level value distribution

C. Major Feature Extraction

The shadow of the vehicle is considered the most important feature in sunny and cloudy conditions. A vehicle with a relatively long shadow is shown in **Fig. 8-(a)**. The Sobel horizontal edge detection result is illustrated in **Fig. 8-(b)**.

(a) (b)

Fig. 8. (a) The source image (b) The Sobel horizontal edge detection result

From observation it can be seen that the area underneath the vehicle is darker than the shadow of the vehicle. The threshold value of this area is obtained by projecting the gray-level value to the *v*-axis, as in **Fig. 9-(a)**, by

$$(V_1,\ldots,V_n)=(\sum_{i=1}^{m}B(u_i,v_1),\ldots,\sum_{i=1}^{m}B(u_i,v_n)) \tag{17}$$

where $B(u_m, v_n)$ and $(V_1,\ldots,V_n)$ are the binary values and the projection vectors, respectively. The projection result is shown in **Fig. 9-(b)**. The maximum element of V is given by $V_{\max}=\max\{V_i \mid 1\le i\le n\}$. One-fourth of $V_{\max}$ is chosen as the threshold value B_{th}. The blue region is re-projected so that the projection vector $V_i > B_{th}$ is set to 255 and the others are 0. The positions of the vectors at projection value 255 are recorded. If the length of the continuous recorded projection vectors is large enough to be considered a vehicle, the bottom row of the continuous projection vectors is identified as the bottom of the vehicle. The position of the vehicle is obtained as shown in **Fig. 9-(c)**. The lower red line is the original detection results using the Sobel edges, while the yellow line is the fixed result of vehicle detection.

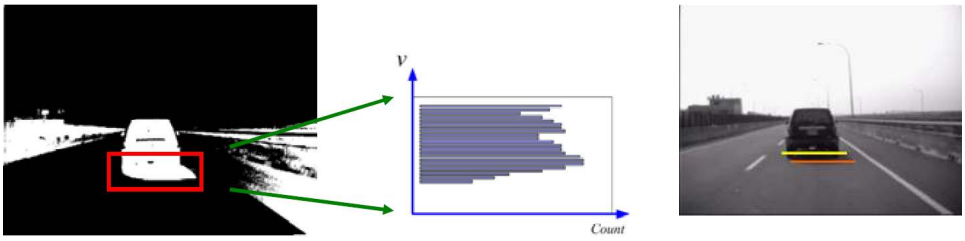

(a) (b) (c)

Fig. 9. (a) The binary map (b) The projection result (c) The detection result

D. Vertical Edge Pair Detection

Vertical edge pair is also an important feature in the vehicle detection process. A truck, a sedan, a dark-colored car, and a light-colored car all have a pair of vertical edges. This procedure is applied for most weather conditions. After Major Feature Extraction, the location of the vehicle can be detected. The ROI of a pair of vertical edges detection is picked from the bottom of the vehicle as shown in **Fig. 10-(a)**, and the vertical edges within ROI are projected onto the *u* axis by

$$(U_1,\ldots,U_m)=(\sum_{i=1}^{n}V(u_1,v_i),\ldots,\sum_{i=1}^{n}V(u_m,v_i)) \tag{18}$$

where $V(u_m, v_n)$ and $(U_1,\ldots,U_m)$ are the binary vertical values and the projection vectors, respectively. An histogram of the Sobel vertical edge is depicted in **Fig. 10-(b)**. The maximum element of U is $U_{\max}=\max\{U_i \mid 1\le i\le m\}$. Half of U_{max} is chosen as the threshold value to indicate the major vertical edge. In **Fig. 10-(c)**, the edge histogram in the candidate block gives two peaks, which indicate the vehicle side boundaries.

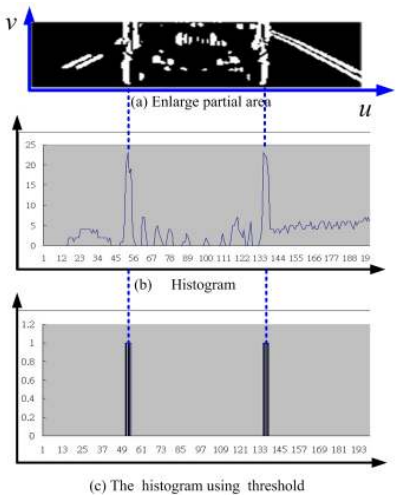

Fig. 10. Vertical edge pair detection

E. Time and Spatial Constraint

If the vehicle is detected in Single Mode, the position of the vehicle is stored. As the movement of a vehicle in a short period of time is very small, the variation of the vehicle position in the image is negligible. Otherwise, the object is considered to be noise.

3.2 Algorithms for Blind Spot Collision Warning

To avoid possible collisions within blind spot areas, blind spot collision warning was developed to overcome this safety driving drawback. Just like the detection process for the front and rear, the lane information is used to provide bounds for the detection area and the relationship between the image coordinate and the world coordinate is used to obtain the estimated distance. However, there are still some different conditions between them. One is the pan angle of the camera, and the other is the situation of the closing vehicle. The pan angle β exists due to the camera setting for blind spot detection. The view image is different from the one in the front and at the rear, and the formulas also have a little difference, as explained in Section 2. When the vehicle in the side lane is about to overtake the host vehicle, the shape in the image is incomplete. In this situation, the vehicle is defined as a closing vehicle. Therefore, the detection flow is designed to detect the near lane marking first, and then estimate the farther lane to get a bounded detection area, as shown in **Fig. 11**. Next, the existence of the closing vehicle is checked. Finally, the approaching vehicle has to be assessed in order to enable the driver to know the corresponding distance.

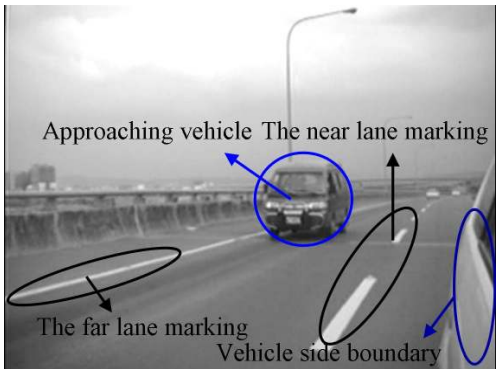

Fig. 11. The near lane marking and the far lane marking

A. Detection of Closing Vehicle in the Neighboring Lane

When there is a closing vehicle in the neighboring lane, a large gray area with intensity different from that of the road will appear. Therefore, an RH area is arranged, as in **Fig. 12**, to estimate the gray intensity histogram of the road surface. In order to avoid being influenced by the white lane marking, we set RH_Width > RH_Height. The gray intensity histogram is shown in **Fig. 13**. The largest value for the gray intensity is denoted I_{RHmax} and the region $R \in [I_{\mathrm{RHmax}} - 30,\ I_{\mathrm{RHmax}} + 30]$ is assigned as the gray intensity region of the road surface. The gray intensity of the pixels, $I(u, v)$, in LV_1 and LV_2 will be checked against R and the ratio, $\rho = P/N$, is obtained, where P indicates the number of the pixels and $I(u, v) \notin R$ and N signify the total pixels in LV_1 and LV_2, respectively. When $\rho_{LV1} > 0.8$ or $\rho_{LV2} > 0.8$; it signifies that there is a closing vehicle in the neighboring lane.

Fig. 12. The region checked in order to detect a vehicle in the neighboring lane

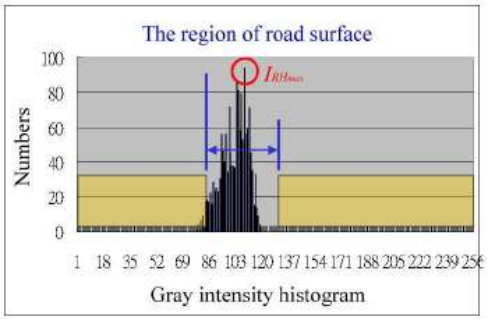

Fig. 13. The gray intensity histogram of the RH area

B. Far Lane Marking Detection and Approaching Vehicle Detection and Distance Estimation

If there is no closing vehicle in the neighboring lane, then the far lane marking detection starts. The ROI of the far lane marking is set up by the detected near lane marking, as illustrated in **Fig. 14**. In Section 2, the near lane marking straight line was described as $v = a_0 + a_1u$. From (13), the lane width in world space, W, can be mapped on to the image plane as u. Consequently, the ROI of the far lane marking can be set up as in **Fig. 14**. The straight line $v = a_2 + a_3u$ of the predicted ROI can be obtained by estimating the horizontal distance from the near lane marking to the far lane marking in the image.

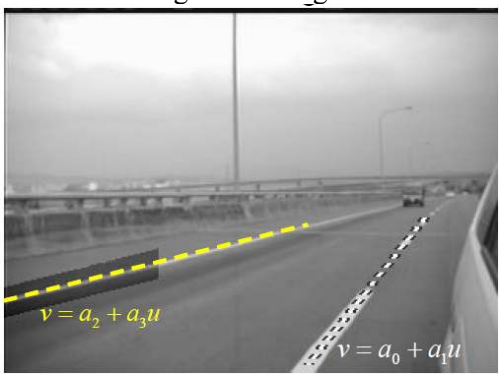

Fig. 14. Adaptive ROI of the far lane marking

In **Fig. 15**, the vanishing point A is at the intersection of the two lane markings. Three virtual lines in the neighboring lane can be determined. M_1, M_2, and M_3 are the midpoints of $\overline{BC}$, $\overline{BM_1}$, and $\overline{BM_2}$, respectively. If some horizontal edge pixels are detected on the three virtual lines, the density of the horizontal edge pixels in D_hBox (**Fig. 16**) is estimated.

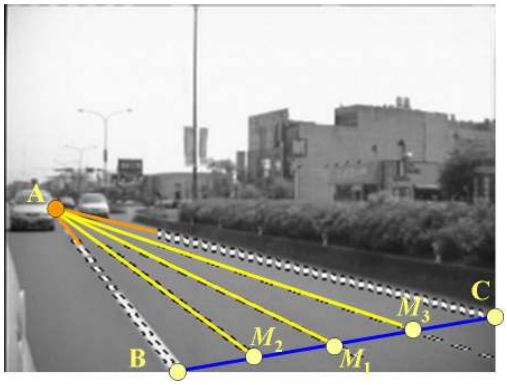

Fig. 15. The virtual lines in the neighboring lane

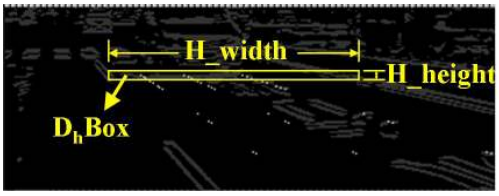

Fig. 16. The region of horizontal edge pixels checked

H_width is the width of the lane and H_height is three pixels high if the density of the horizontal edge pixels in D_hBox is sufficiently large. In **Fig. 17**, V_width is the width of the lane width and V_height is half of V_width. If the density of the vertical edge pixels in D_vBox is sufficiently large, it implies that there exists an approaching vehicle in the neighboring lane. Consequently, the candidate area is processed with major feature extraction, vertical edge pair detection, and time and spatial constraint to get more detailed information on the vehicle.

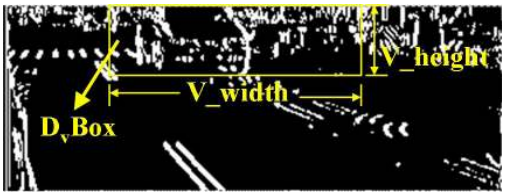

Fig. 17. The region of vertical edges checked

After the position of the vehicle has been ascertained, the estimated distance between the host vehicle and the vehicle approaching from the side lane is calculated. The real distance D from the detected vehicle to the host vehicle, shown in **Fig. 18**, is estimated using the Cosine rule, where D_{cv} is the distance between the detected vehicle and the camera, and d indicates the distance from the side mirror to the back side of the vehicle. The information is used to trigger an alarm that alerts the driver when the distance is too close.

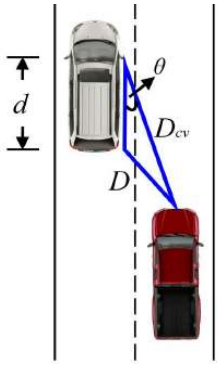

Fig. 18. Distance from the detected vehicle to our system

3.3 Warning Strategy and Surroundings Monitoring

To provide the vehicle surrounding monitoring function, our system has to collect information that includes the lateral offset and the estimated distance of the front, rear, and blind spots from the detection results. After the system receives the detection results, the following warning criteria are used to decide on the proper warning messages to use.

$$D_{front/rear} < \frac{1}{2} D_{speed} \tag{19}$$

$$D_{blindspot} < 10 \tag{20}$$

The alarm for the front and rear collision is decided by (19), where $D_{front/rear}$ is the estimated distance to the vehicles in the front or rear, and D_{speed} is the distance corresponding to the current speed of the host vehicle. For example, if the speed is 90 km/hr, D_{speed} is set as 90 m. This rule implies that if $D_{front/rear}$ is less than one-half of D_{speed} the system will raise the alarm to warn the driver. If the host vehicle is not changing lanes, the approaching vehicles in the blind

spots are no immediate threat. Therefore, to prevent a possible collision when the driver changes lanes without noticing the approaching vehicles in the blind spots, the warning rule for blind spots is decided by (20), where $D_{blindspot}$ is the estimated distance to the vehicles in the blind spots and the threshold is set to 10 m. **Fig. 19** gives the flowchart for the warning strategy.

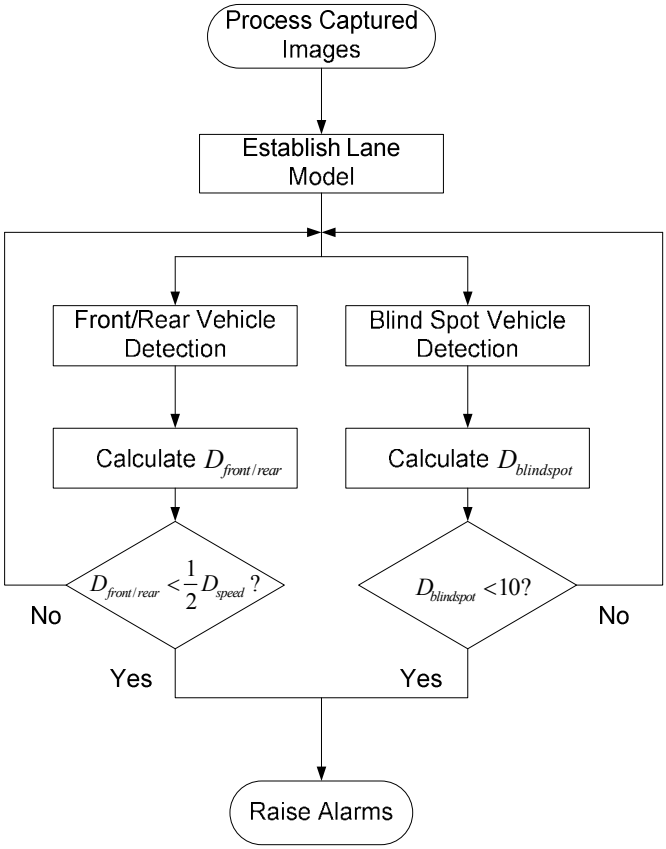

Fig. 19. The flowchart for the warning strategy

4. Implementation Results

This section describes the implementation details and the experimental results obtained. All functionalities were successfully implemented and installed in an experimental car. Four cameras were installed: one at the front windshield, another at the back windshield, and one on each of the side mirrors, as shown in **Fig. 20**. The system prototype was implemented on a TI DM642 platform that had a 600 MHz DSP processor. Images were captured from the cameras and inputted to the DSP to be processed for various purposes. The processing performance for an image size of 352 × 240 (CIF) achieved 30 frames per second (FPS). The experimental results of each function are described below.

(a) Front (b) Rear (c) Left (d) Right

Fig. 20. Cameras in the car

The algorithms for vehicle detection on actual roads under various lighting and weather conditions were verified. The detection results for lane markings and vehicles in front and to the rear are shown in **Fig. 21**. **Fig. 21(a)-(c)** show the various forms of interference that were on the road surface, such as texts, on-bridge joint, and shadow under the bridge. The system overcame the interferences and detected vehicles correctly. At night, the interference not only included the text on the road, but also the headlights of other vehicles. The detection results are shown in **Fig. 21(d)-(f)**. As shown in **Fig. 21-(g)** and **21-(h)**, it was raining heavily during the day on Highway No. 1 in Taiwan. Our system successfully overcame the interference caused by the wipers, drops of water on the windshield, and light reflected off the road surface. In addition, it also operated properly on curved roads. Because the lane markings are modeled using parabolic polynomial functions, the detected lines can fit real curvatures properly, as illustrated in **Fig. 21-(i)**.

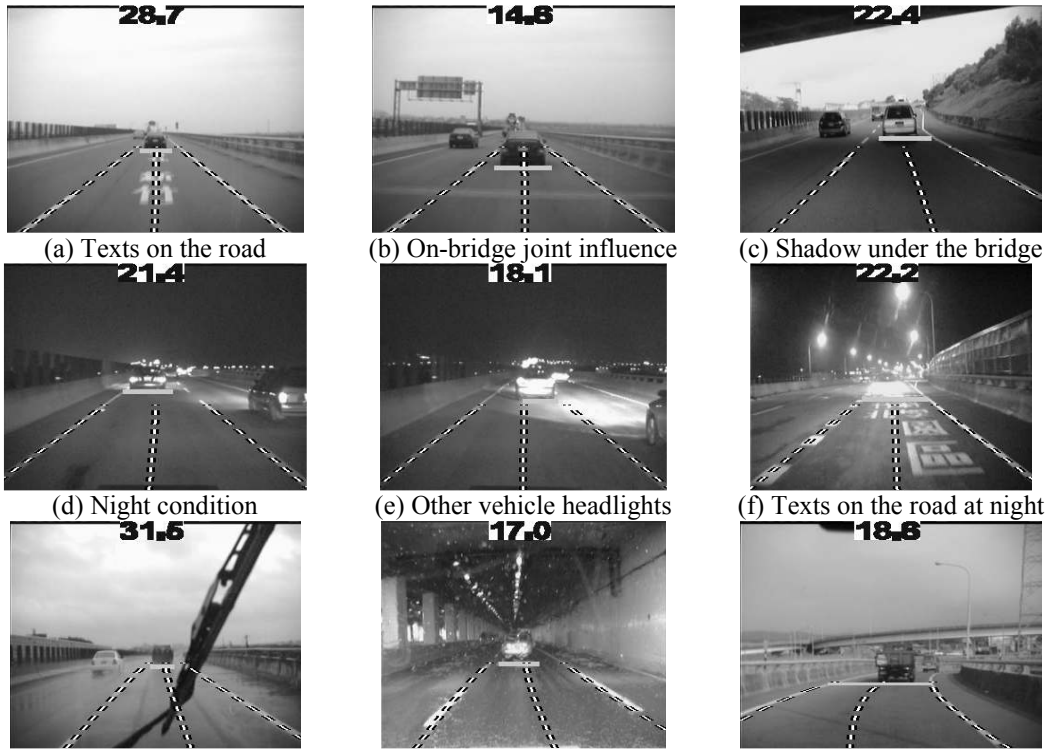

(a) Texts on the road (b) On-bridge joint influence (c) Shadow under the bridge

(d) Night condition (e) Other vehicle headlights (f) Texts on the road at night

(g) Rainy day condition with wiper interference (h) Drops of water on the windshield (i) Curved road

Fig. 21. Detection results in front and at the rear under various conditions

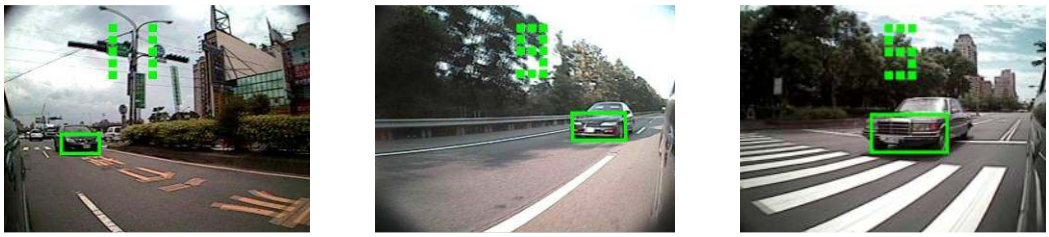

(a) Texts on the road (b) Shadow of trees (c) Zebra crossing on road

(d) Tailed shadow (e) Headlights reflected on a rainy day (f) Rainy day with drops of water

Fig. 22. Detection results in the blind spots under various conditions

Fig. 22 demonstrates the detection results in the blind spots under various lighting and weather conditions. **Fig. 22(a)-(d)** show the various forms of interference on the road surface, such as texts, the shadow of trees, zebra crossing, and tailed shadow of closing vehicles. On a rainy day, the headlights reflecting off the road surface and drops of water are major forms of interference, as illustrated in **Fig. 22-(e)** and **22-(f)**. However, the vehicle detection algorithms successfully gave the desired outcomes at 30 FPS.

To evaluate the accuracy of the estimated distances, traffic cones were placed away from the vehicle as a reference to measure real distances. The measured distances in the front/rear and blind spot ranged from 20 to 60 m and from 5 to 20 m, respectively. The experimental results of real and estimated distances with average error, standard deviation, and maximum error for each distance are summarized in **Table 1** and **Table 2**. Furthermore, to evaluate the vehicle detection ability, we conducted experiments covering a variety of lighting and weather conditions (day, night, and rainy), and selected Highway No. 1 in Taiwan as the test scene. On average, the correctness ratio for vehicle detection was more than 93%. **Table 3** shows the detection ratio for the front, rear, and blind spots under the different conditions. Detection ratio is defined as true positive / (true positive + false negative), where true positive means the number of frames for which the lane markings or vehicles are correctly detected, and false negative represents the number of frames for which lane markings or vehicles exist but are not detected. Both detection ratios of lane markings and vehicles were above 90%. The percentage of lane marking detection was even higher at 99%. On the other hand, the average detection ratio in the blind spot was approximately 95%.

Table 1. Distance estimation in front and at the rear

Real Distance (m)	Estimated Distance (m)	Average Error (%)	Standard Deviation (m)	Maximum Error (m)
20	20.45	2.25	0.077	0.53
30	30.97	3.23	0.173	1.16
40	41.85	4.63	0.308	2.18
50	52.74	5.48	0.481	3.23
60	64.05	6.75	0.692	4.81

Table 2. Distance estimation in the blind spots

Real Distance (m)	Estimated Distance (m)	Average Error (%)	Standard Deviation	Maximum Error
5	5.16	3.2	0.005	0.17
10	10.21	2.1	0.019	0.23
15	15.37	2.47	0.044	0.42
20	20.53	2.65	0.078	0.62

Table 3. Detection ratio in front, at the rear and in blind spots under the different conditions.

	Front and Rear		Blind Spot	
Weather	False Negative / True Positive	Detection Ratio	False Negative / True Positive	Detection Ratio
Daytime	31/1018	97.04%	38/2500	98.48%
Rain	85/1038	92.43%	126/2000	93.7%
Nighttime	59/1024	94.55%	123/2500	95.08%
Total	175/3080	94.62%	287/7000	95.90%

The performance of vehicle detection in front and at the rear, and in the blind spots is compared with other approaches in **Table 4** and **Table 5**, respectively. The test scenario in the comparison was Highway No. 1, in Taiwan, and a driver driving for 30 min in the daytime. For vehicle detection in front and at the rear, Kim et al. [24] also used lane information to assist the vehicle detection process, while Sun et al. [21] used the effective features of the vehicle. The results show that vehicle detection ability is enhanced by adding lane information. However, without the assistance of the camera model, both works cannot provide distance information to drivers. Similarly, the performance of our proposed system in the blind spot was compared with the vertical-edge based method [28], and the region-based method [34], respectively. The results show that our proposed system not only provides better performance, but also can offer distance information to the driver. In consequence, the experimental results above reveal that our proposed approach works well for vehicle detection in front, at the rear, and in the blind spots.

Table 4. Comparisons of vehicle detection in front and at the rear.

Scenario	Test period	Proposed	Kim et al. [24]	Sun et al. [21]
Highway in the daytime	30 min	97.04%	96.12%	94.47%

Table 5. Comparisons of vehicle detection in the blind spots.

Scenario	Test period	Proposed	Lin et al. [28]	Cayir et al. [34]
Highway in the daytime	30 min	98.48%	81.94%	82.35%

5. Conclusion

This research proposed a vision-based collision warning system that detects and monitors surrounding vehicles in order to keep drivers aware as to the status of their surroundings. Vehicle detection is designed not only for the front and rear, but also for the blind spots. The distances to the surrounding vehicles are all estimated to determine the possibility for collisions. The system notifies drivers if they are too close to other vehicles, and reduces the danger caused by the blind spots when they are changing lanes. Our algorithm uses camera and lane models to derive the distances from the image coordinates to the world coordinates. Using

different parameters, i.e., pan angles, the formula can be used for the front, rear, and side views. This significantly reduces system complexity by reusing the same basic part in the algorithm for different purposes. The developed functions were fully implemented on an embedded platform and tested in a real environment. The performance of our vehicle detection system was tested under various conditions on different road types. It was successfully verified over hundreds of kilometers on Highway No.1 and Expressway No. 68 in Taiwan. This confirms that our algorithm is robust in varied environments. In the future, the addition of driving status recorders and remote surveillance of the driver are interesting extensions for driving safety.

References

[1] M. W. Ryu, S. H. Cha, J. G. Koh, S. Kang and K. H. Cho, "Position-based routing algorithm for improving reliability of inter-vehicle communication," *KSII Transactions on Internet and Information Systems*, vol.5, no.8, pp.1388-1403, Aug.2011. Article (CrossRef Link).

[2] E. Dickmanns, "The development of machine vision for road vehicles in the last decade," in *Proc. IEEE Intelligent Vehicle Symp.*, vol.1, pp.268-281, Jun.2002. Article (CrossRef Link).

[3] M. Bertozzi and A. Broggi, "GOLD: A parallel real-time stereo vision system for generic obstacle and lane detection," *IEEE Trans. Image Processing*, vol.7, pp.62-81, Jan.1998. Article (CrossRef Link).

[4] M. Bertozzi, A. Broggi, G. Conte and A. Fascioli, "Obstacle and lane detection on ARGO," in *Proc. IEEE Intelligent Vehicle Symp.*, pp.1010-1015, Nov.1997. Article (CrossRef Link).

[5] M. Herbert, "Active and passive range sensing for robotics," in *Proc. IEEE Int'l Conf. Robotics and Automation*, vol.1, pp.102-110, 2000. Article (CrossRef Link).

[6] S. J. Park, T. Y. Kim, S. M. Kang and K. H. Koo, "A novel signal processing technique for vehicle detection radar," in *Proc. IEEE Microwave Symp. Digest*, pp.607-610, 2003. Article (CrossRef Link).

[7] C. C. Wang, C. Thorpe and A. Suppe, "Ladar-based detection and tracking of moving objects from a ground vehicle at high speeds," in *Proc. IEEE Intelligent Vehicles Symp.*, pp.416-421, Jun.2003. Article (CrossRef Link).

[8] R. Chellappa, G. Qian and Q. Zheng, "Vehicle detection and tracking using acoustic and video sensors," in *Proc. IEEE Int'l Conf. Acoustics, Speech, and Signal Processing*, pp.793-796, 2004. Article (CrossRef Link).

[9] W. S. Wijesoma, K. R. S. Kodagoda and A. P. Balasuriya, "Road-boundary detection and tracking using ladar sensing," *IEEE Trans. Robotics and Automation*, vol.20, no.3, pp.456-464, Jun.2004. Article (CrossRef Link).

[10] S. T. Sheu, J. S. Wu, C. H. Huang, Y. C. Cheng and L. W. Chen, "DDAS: Distance and direction awareness system for intelligent vehicles," *Journal of Information Science and Engineering*, vol.23, pp.709-722, 2007.

[11] T. Matsumoto, N. Yoshitsugu and Y. Hori, "Toyota advanced safety vehicle (Toyota ASV)," *TOYOTA Technical Review*, vol.46, pp.57-64, 1996.

[12] L. M. Bergasa, J. Nuevo, M. A. Sotelo, R. Barea and M. E. Lopez, "Real-time system for monitoring driver vigilance," *IEEE Trans. Intelligent Transportation System*, vol.7, pp.63-77, Mar.2006. Article (CrossRef Link).

[13] T. Hayami, K. Matsunaga, K. Shidoji and Y. Matsuki, "Detecting drowsiness while driving by measuring eye movement - a pilot study," in *Proc. IEEE Intelligent Transportation Systems*, pp.156-161, Sep.2002. Article (CrossRef Link).

[14] R. Okada, Y. Taniguchi, K. Furukawa and K. Onoguchi, "Obstacle detection using projective invariant and vanishing lines," in *Proc. IEEE Computer Vision*, vol.1, pp.330-337, 2003. Article (CrossRef Link).

[15] R. Okada and K. Onoguchi, "Obstacle detection based on motion constraint of virtual planes," in *Proc. IEEE/RSJ Intelligent Robots and System*, vol.1, pp.61-66, Sep.2002. Article (CrossRef Link).

[16] C. Demonceaux, A. Potelle and D. Kachi-Akkouche, "Obstacle detection in a road scene based on motion analysis," *IEEE Trans. Vehicular Technology*, vol.53, pp.1649-1656, Nov.2004. Article (CrossRef Link).
[17] H. Mallot, H. Bulthoff, J. Little and S. Bohrer, "Inverse perspective mapping simplifies optical flow computation and obstacle detection," *Biol. Cybern.*, vol.64, no.3, pp.177-185, 1991. Article (CrossRef Link).
[18] G. Zhao and Y. Shini'chi, "Obstacle detection by vision system for an autonomous vehicle," in *Proc. IEEE Intelligent Vehicle Symp.*, pp.31-36, 1993. Article (CrossRef Link).
[19] C. Knoeppel, A. Schanz and B. Michaelis, "Robust vehicle detection at large distance using low resolution cameras," in *Proc. IEEE Intelligent Vehicle Symp.*, pp.267-172, 2000. Article (CrossRef Link).
[20] M. Suwa, "A stereo-based vehicle detection method under windy conditions," in *Proc. IEEE Intelligent Vehicle Symp.*, pp.246-249, 2000. Article (CrossRef Link).
[21] Z. Sun, G. Bebis and R. Miller, "Monocular precrash vehicle detection: features and classifiers," *IEEE Trans. image processing*, vol.15, no.7, Jul.2006. Article (CrossRef Link).
[22] Z. Sun, G. Bebis and R. Miller, "Quantized wavelet features and support vector machines for on-road vehicle detection," in *Proc. Control, Automation, Robotics and Vision International Conference*, vol.3, pp.1641-1646, Dec.2002. Article (CrossRef Link).
[23] A. Kuehnle, "Symmetry-based recognition for vehicle rears," *Pattern Recognition Letters*, vol.12, pp.249-258, 1991. Article (CrossRef Link).
[24] S. Y. Kim, S. Y. Oh, J. K. Kang and Y. W. Ryu, "Front and rear vehicle detection and tracking in the day and night times using vision and sonar sensor fusion," in *Proc. IEEE Intelligent Robots and Systems Conference*, pp.2173-2178. Aug.2005. Article (CrossRef Link).
[25] J. Crisman and C. Thorpe, "Color vision for road following," in *Proc. SPIE Conf. Mobile Robots*, pp.246-249, 1988.
[26] S. D. Buluswar and B. A. Draper, "Color machine vision for autonomous vehicles," *Int'l J. Eng. Applications of Artificial Intelligence*, vol.1, no.2, pp.245-256, 1998. Article (CrossRef Link).
[27] H. Mori and N. Charkai, "Shadow and rhythm as sign patterns of obstacle detection," in *Proc. Int'l Symp. Industrial Electronics*, pp.271-277, 1993. Article (CrossRef Link).
[28] M. Lin and X. Xu, "Multiple vehicle visual tracking from a moving vehicle," in *Proc. International Conference on Intelligent System Design and Applications*, pp.373-378, 2006. Article (CrossRef Link).
[29] N. Matthews, P. An, D. Charnley and C. Harris, "Vehicle detection and recognition in greyscale imagery," *Control Eng. Practice*, vol.4, pp.473-479, 1996. Article (CrossRef Link).
[30] M. Betke, E. Haritaglu and L. Davis, "Real-time multiple vehicle detection and tracking from a moving vehicle," *Machine Vision and Applications*, vol.12, no.2, pp.69-83, 2000. Article (CrossRef Link).
[31] N. Srinivasa, "Vision-based vehicle detection and tracking method for forward collision warning in automobiles," in *Proc. IEEE Intelligent Vehicle Symp.*, pp.626-631, 2002. Article (CrossRef Link).
[32] T. Bucher, C. Curio, J. Edelbrunner, C. Igel, D. Kastrup, I. Leefken, G. Lorenz, A. Steinhage and W. von Seelen, "Image processing and behavior planning for intelligent vehicles," *IEEE Trans. Industrial Electronics*, vol. 50, no.1, pp.62-75, 2003. Article (CrossRef Link).
[33] S. J. Wu, H. H. Chiang, J. W. Perng, C. J. Chen, B. F. Wu and T. T. Lee, "The heterogeneous systems integration design and implementation for lane keeping on a vehicle," *IEEE Trans. Intelligent Transportation Systems*, vol.9, pp.246-263, 2008. Article (CrossRef Link).
[34] B. Cayir and T. Acarman, "Low cost driver monitoring and warning system development," in *Proc. IEEE Intelligent Vehicle Symposium*, pp.94-98, Jun.2009. Article (CrossRef Link).

Bing-Fei Wu received the B.S. and M.S. degrees in control engineering from National Chiao Tung University (NCTU), Hsinchu, Taiwan, in 1981 and 1983, respectively, and the Ph.D. degree in electrical engineering from the University of Southern California, Los Angeles, in 1992. Since 1992, he has been with the Department of Electrical Engineering, where he is a Professor in 1998 and promoted as Distinguished Professor in 2010. He serves as the Director of the Institute of Electrical and Control Engineering, NCTU since 2011. He has been involved in the research of Intelligent Transportation Systems for many years and leads a research team to develop the first Taiwan smart car, TAIWAN *i*TS-1, with autonomous driving and active safety system. He has been elevated as a Fellow of the IEEE 2012 for his contributions to intelligent transportation and multimedia systems. He is also an IET Fellow. His current research interests include image recognition, vehicle driving safety, intelligent control, intelligent transportation systems, multimedia signal analysis, embedded systems and chip design.

Ying-Han Chen was born in Tainan, Taiwan in 1981. He received the B.S. and M.S. degrees in electrical engineering from National Central University, Jhongli, Taiwan, in 2003 and 2006, respectively. He is currently working toward the Ph.D. degree in electrical engineering at National Chiao Tung University, Hsinchu, Taiwan. His research interests include networking, embedded systems, and digital signal processing.

Chih-Chung Kao was born in Ping-Tong, Taiwan in 1982. He received the B.S. degree in electrical engineering from National Taiwan Ocean University, Keelung, Taiwan, in 2004, and the M. S. degree in industrial education from National Taiwan Normal University, Taipei, Taiwan, in 2006. He is currently working for his Ph. D degree in National Chiao Tung University, Hsinchu, Taiwan. His research interest includes image processing, pattern recognition, statistical learning, and intelligent transportation system.

Yen-Feng Li was born in Taitung, Taiwan in 1976. He received the B.S. degree in Electronic Engineering from National Taiwan University of Science And Technology, Taipei, Taiwan in 2007, and the M. S. degree in Electronic Engineering from National Chin-Yi University of Technology, Taichung, Taiwan, in 2009. His research interests include image processing, embedded systems, and intelligent transportation system.

Chao-Jung Chen was born in TaoYuan, Taiwan in 1977. He received his B.S. and M.S. degree in the Institute of Mechanical Engineering from Huafan University, Taiwan, in 1999 and 2001, respectively, and the Ph.D. degree in electrical and control engineering from the National Chiao-Tung University (NCTU), Hsinchu, in 2006. He is currently a Research Assistant Professor in the Department of Electrical and Control Engineering, NCTU. His research interest is real-time image processing in intelligent transportation systems.